

Monitoring Catalytic 2-Propanol Oxidation over Co₃O₄ Nanowires via In Situ Photoluminescence Spectroscopy

*Julian Klein,[†] Laura Kampermann,[†] Jannik Korte,[†] Maik Dreyer,[‡] Eko Budiyanto,[§] Harun
Tüysüz,[§] Klaus Friedel Ortega,[⊥] Malte Behrens,^{‡, ⊥} and Gerd Bacher^{†, *}*

[†] Werkstoffe der Elektrotechnik and CENIDE, Universität Duisburg-Essen, Bismarckstraße 81,
47057 Duisburg, Germany, E-Mail: gerd.bacher@uni-due.de

[‡] Faculty for Chemistry, Inorganic Chemistry and CENIDE, Universität Duisburg-Essen, 45141
Essen, Germany

[§] Department of Heterogeneous Catalysis, Max-Planck-Institut für Kohlenforschung, Mülheim an
der Ruhr, 45470, Germany

[⊥] Institute for Inorganic Chemistry, Christian-Albrechts-Universität zu Kiel, 24118 Kiel, Germany

ABSTRACT

Spectroscopic methods enabling real-time monitoring of dynamic surface processes are a prerequisite for identifying how a catalyst triggers a chemical reaction. We present an *in situ* photoluminescence spectroscopy approach for probing the thermo-catalytic 2-propanol oxidation over mesostructured Co_3O_4 nanowires. Under oxidative conditions, a distinct blue emission at ~ 420 nm is detected that increases with temperature up to 280°C , with an intermediate maximum at 150°C . Catalytic data gained under comparable conditions show that this course of photoluminescence intensity precisely follows the conversion of 2-propanol and the production of acetone. The blue emission is assigned to the radiative recombination of unbound acetone molecules, the $n \leftrightarrow \pi^*$ transition of which is selectively excited by a wavelength of 270 nm. These findings open a pathway for studying thermo-catalytic processes via *in situ* photoluminescence spectroscopy thereby gaining information about the performance of the catalyst and the formation of intermediate products.

MAIN TEXT

To develop and optimize suitable and effective catalytic materials, it is highly beneficial to understand catalytic processes as completely as possible. This includes knowledge of active surface sites and occurring reaction/intermediate products as well as an understanding of the underlying reaction mechanism for being able to design a catalyst with optimal activity and selectivity.¹⁻⁴ However, since the surface of a working catalyst is exposed to permanent changes depending on adsorbates or the surrounding reaction conditions, these informations can only be obtained by *in situ* methods.^{1,4-8}

For the examination of heterogeneous gas phase catalysis over metal oxides, optical spectroscopy, including Raman, infrared (IR), or UV/Vis absorption measurements, is an established methodology.^{7,9-16} The combination of optical methods enables access to electronic and structural information about the working catalyst and its surface as well as the chemical reaction, the latter, e.g., via vibrational signatures of reaction products or intermediates.¹⁵ Using photons that in contrast to electrons and ions do not require any special vacuum conditions as a probe and as a detection signal, molecules and the catalyst bulk can be examined barely influencing the catalytic process.^{9,15,17}

An optical spectroscopy tool, which has so far hardly been used for *in situ* investigations of catalytic gas phase processes (only a few studies on photocatalysis exist^{18,19}) is photoluminescence (PL) spectroscopy. With PL spectroscopy, electronic transitions of metal oxide catalysts,^{20,21} active surface sites^{22,23} or molecules at the metal oxide gas phase interface^{24,25} can be excited and detected. PL spectroscopy shows a high sensitivity to smallest concentrations, even for fluorescent

molecules with low quantum yields.⁹ For acetone molecules (PL quantum yield ~0.12%) a detection limit of 65 ppm was determined in an air gas flow.²⁶ By using specific excitation wavelengths reaction products as well as the catalyst itself including its active surface centers can be selectively excited and their signals separately detected.²² In this way, a specific sub-component of a catalytic process can be monitored with high sensitivity and quite locally at the catalyst surface without affecting the catalytic process.

In this work we report on a study of thermo-catalytic gas phase 2-propanol oxidation to acetone over mesostructured Co_3O_4 nanowires using *in situ* PL spectroscopy. The 2-propanol oxidation is an established standard reaction for determining the performance of catalysts and $\text{Co}_x\text{Fe}_{3-x}\text{O}_4$ nanostructures have recently shown their suitability as an effective catalyst for the formation of acetone with high activity and selectivity.²⁷⁻²⁹ We demonstrate that a blue emission is observable under UV irradiation with rising temperature in a 2-propanol/ O_2/N_2 gas flow. By performing additional catalytic tests with gas chromatography under comparable thermo-catalytic conditions, we show that this blue PL signal follows the conversion of 2-propanol to acetone precisely. A model describing the underlying mechanism is presented.

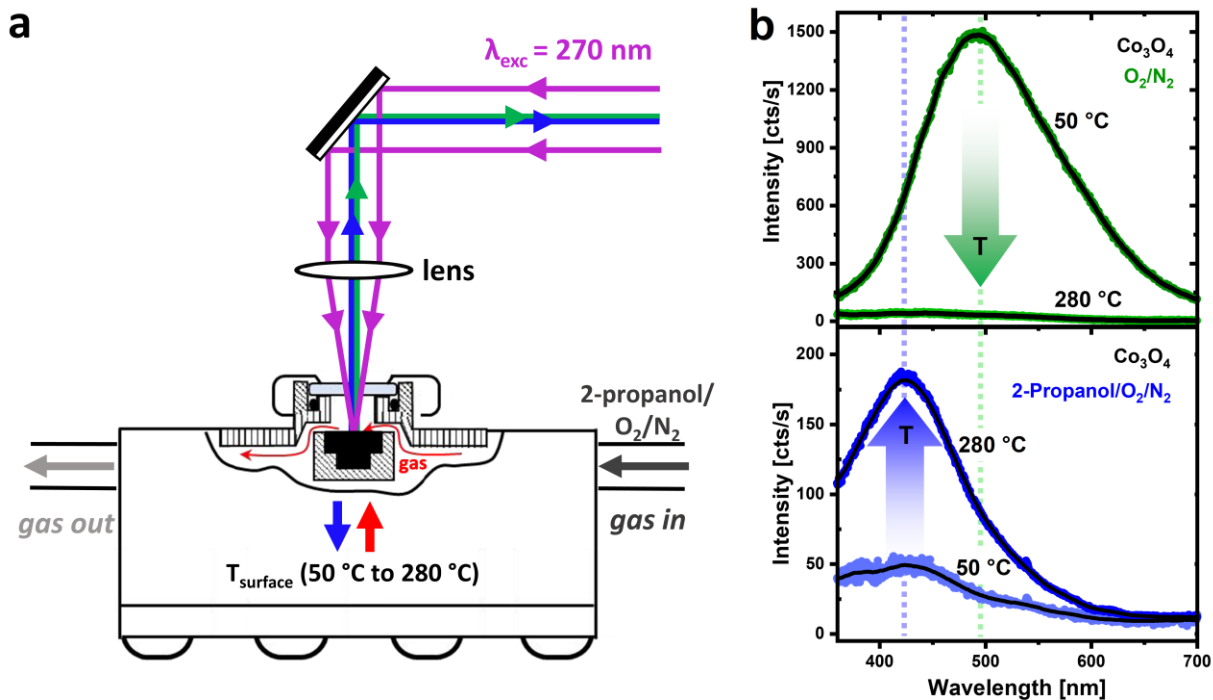


Figure 1. (a) Optical measurement setup for *in situ* photoluminescence investigations of the gas phase 2-propanol oxidation. (b) Top: Emission spectrum of Co_3O_4 nanowires during temperature programmed oxidation (TPO) for surface activation at temperatures of 50 °C and 280 °C in an O_2/N_2 gas flow. Bottom: Emission spectrum of Co_3O_4 nanowires during 2-propanol oxidation at temperatures of 50 °C and 280 °C in a 2-propanol/ O_2/N_2 gas flow after TPO. All spectra were detected under UV excitation ($\lambda_{\text{exc}} = 270 \text{ nm}$, $\rho = 7 \mu\text{J}/\text{cm}^2$).

Well-ordered mesostructured Co_3O_4 with nanowire morphology were synthesized via the nanocasting method as described previously.^{30,31} The structural and textural characterization were conducted by high-resolution transmission electron microscopy (HR-TEM), X-ray diffraction (XRD), nitrogen physisorption and Raman measurements and the results are presented in Figure S1 (details are provided in the Supporting Information). To examine the emission behavior of Co_3O_4 nanowires *in situ* during thermo-catalytic oxidation, a reaction chamber with optical access is used and operated at temperatures of up to 280 °C (Figure 1a). A pulsed frequency-tripled fs-

Ti:sapphire laser ($\lambda_{\text{exc}} = 270 \text{ nm}$) serves as excitation source and is focused on the nanowire powder's surface in the catalyst bed via a mirror-lens system. For catalytic PL-tests, the system is supplied with reaction educts by a 2-propanol/ O_2/N_2 gas stream flowing over the catalyst.

Removal of pre-adsorbed species (e.g., water, carbon dioxide, oxygen) or disturbing reaction products occurring during the catalytic reaction (e.g., acetate species) from the surface is indispensable for heterogeneous catalysis to get access to the oxide surface and free active sites.²⁷

Temperature-programmed oxidation (TPO) in an O_2/N_2 gas flow is therefore carried out before each catalytic PL-test. Its effect on the emission behavior of Co_3O_4 nanowires can be seen in Figure 1b (upper panel). Under UV excitation in an O_2/N_2 gas flow, Co_3O_4 nanowires show a broad emission band between 350 nm and 700 nm with a maximum in the green spectral range (~500 nm). During the TPO step with temperatures of up to 280 °C, the emission decreases continuously and can no longer be detected above a temperature of ~200 °C (Figure S2). A broad green emission was observed in studies of metal oxides such as Al_2O_3 or $\text{Co}_x\text{Fe}_{3-x}\text{O}_4$ as well and assigned to OH groups bound to the catalyst's surface.^{24,32,33} TPO experiments in a gas phase reactor coupled with a micro gas chromatograph show water formation upon heating in the gas flow and thereby verify a decrease in surface coverage with water/OH groups up to a temperature of ~200 °C (Figure S2). Above this temperature the water content in the gas flow hardly changes. If Co_3O_4 nanowires are exposed again to a humid room atmosphere after TPO, the broad green emission is restored, which in turn confirms the adsorbate character of the emission source (Figure S3).

Immediately after TPO, the Co_3O_4 nanowires are examined under thermo-catalytic conditions (Figure 1b, lower panel) without exposure to the atmosphere in between. In a 2-propanol enriched O_2/N_2 gas flow, a new blue emission occurs with a maximum at ~ 420 nm, which, in contrast to the green emission associated with OH groups, increases with temperature. The presence of 2-propanol in the gas flow is a prerequisite for the detection of this blue emission; after TPO no emission is visible in a pure O_2/N_2 gas flow (Figure S4). To determine the cause of the blue emission in more detail, a combination of temperature-dependent *in situ* PL measurements and catalytic tests in the gas phase is carried out (Figure 2).

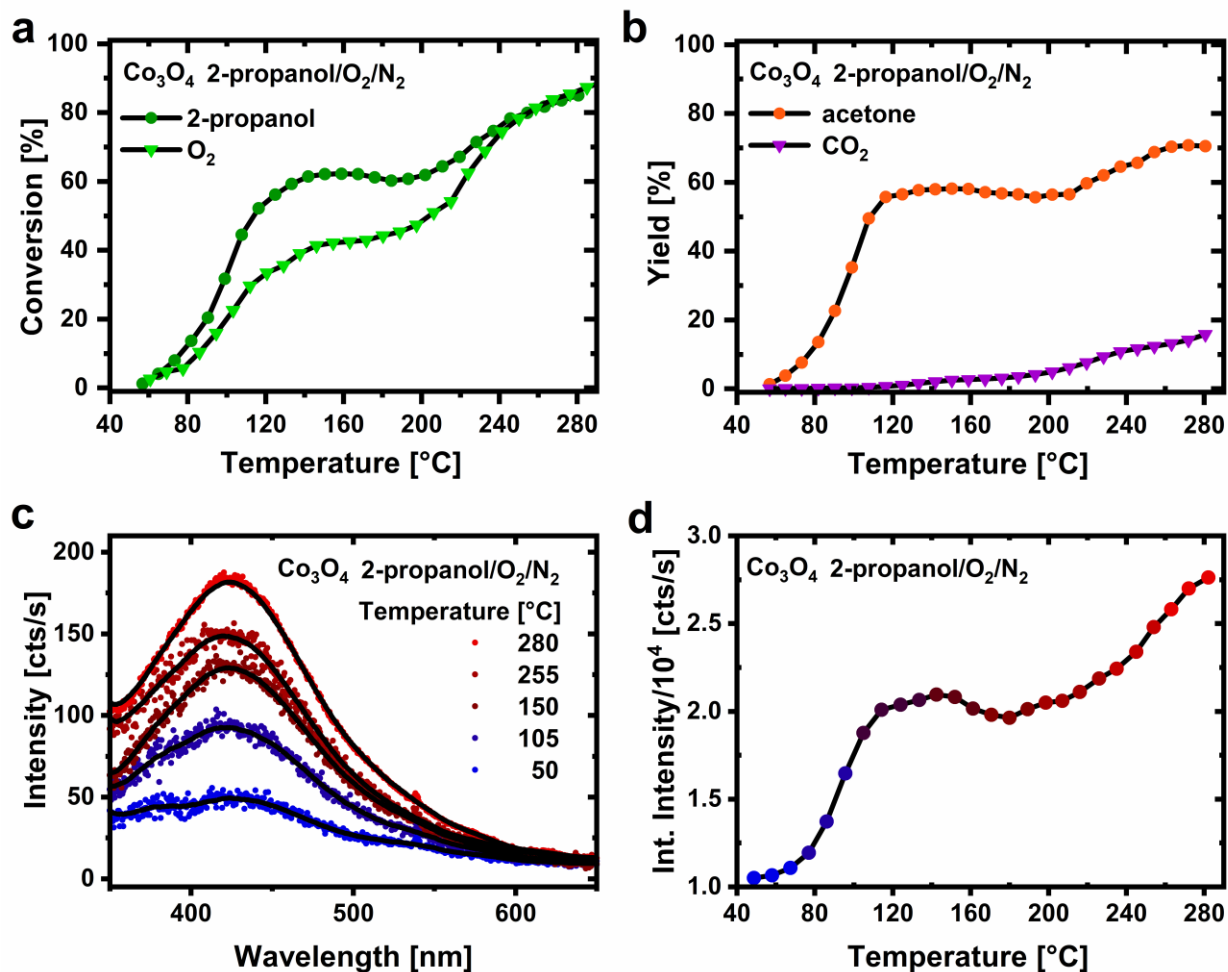


Figure 2. (a) Conversion of 2-propanol and O_2 over Co_3O_4 nanowires and (b) the resulting yields of acetone and CO_2 at temperatures of 50 $^\circ\text{C}$ up to 280 $^\circ\text{C}$ under a constant 2-propanol/ O_2/N_2 gas flow. (c) PL spectra of Co_3O_4 nanowires under UV excitation ($\lambda_{\text{exc}} = 270 \text{ nm}$, $\rho = 7 \mu\text{J}/\text{cm}^2$) and a constant 2-propanol/ O_2/N_2 gas flow at temperatures of 50 $^\circ\text{C}$ up to 280 $^\circ\text{C}$. (d) Corresponding temperature course of the integrated PL intensity.

The catalytic tests are conducted in a setup containing a quartz reactor, the reactor outlet composition is examined using a micro gas chromatograph (see Supporting Information). The conversion of 2-propanol exhibits a first low-temperature maximum at around 150 $^\circ\text{C}$ ($\sim 60\%$),

which is typical for cobalt oxide or cobalt-iron oxides²⁷⁻²⁹ and reaches nearly 85% at high temperatures of 280 °C. In the low-temperature regime, the conversion of 2-propanol can be described by (oxidative) dehydrogenation with acetone as the only reaction product (Figure 2b).²⁷⁻²⁹ With increasing temperature, total oxidation of 2-propanol or acetone²⁹ becomes possible (as well as the oxidation of further compounds, i.e. carbonaceous deposits³⁴), resulting in additional formation of CO₂ (and H₂O). At 280 °C a CO₂ yield of 16% is detected, while the acetone yield starts to saturate with a value of ~70% at high temperatures. In the PL experiments, an increase in the blue emission at 420 nm is observed in a 2-propanol/O₂/N₂ gas flow with rising temperature (Figure 2c, d). Interestingly, in accordance with the conversion of 2-propanol and the formation of acetone, the temperature-dependent PL intensity forms an intermediate maximum at around 150 °C and continues to increase to the maximum temperature of 280 °C afterward. Here, the blue emission follows the conversion of 2-propanol to acetone/CO₂ very precisely (Figure 2a). However, a flattening of the PL intensity above 250 °C, as in the case of the acetone yield (Figure 2b), cannot be detected.

We assign the blue emission to the optical excitation and radiative recombination of acetone molecules. The optical properties of ketones, such as acetone, are determined by its carbonyl group owning an active optical $n \leftrightarrow \pi^*$ transition between neutral, unbound n orbitals localized at the O-atoms and the non-binding π^* orbitals.^{35,36} The process of an electron that is raised from the n to the π^* level with an antiparallel spin alignment of the resulting unpaired electrons is a singlet transition $S_0 \rightarrow S_1$ (Scheme 1) leading to an absorption band between 220 nm and 320 nm with a maximum at around 270 - 280 nm.³⁵ This absorption band was also demonstrated by control experiments with acetone in the liquid phase (Figure S5). Compared to acetone, 2-propanol shows

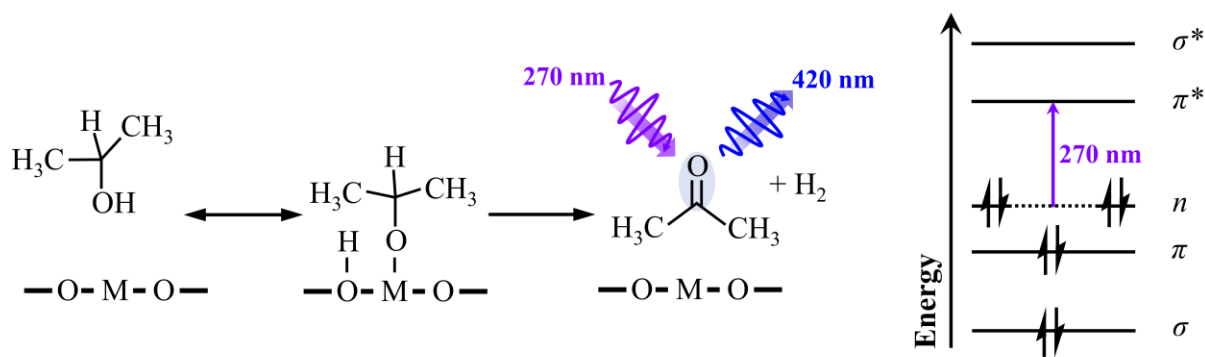
hardly any absorption in this spectral range, which makes a direct excitation of 2-propanol unlikely. Consequently, acetone can be effectively and selectively excited by a wavelength of 270 nm used in this work.

After optical excitation, a radiative recombination occurs either in the form of phosphorescence (transfer to the triplet state T_1 and subsequently radiative recombination to S_0) or by fluorescence ($S_1 \rightarrow S_0$).^{36,37} The $S_1 \rightarrow S_0$ transition results in a broad emission for acetone between 300 and 550 nm with a maximum at 400 - 420 nm.^{35,38-40} The large width and the strong Stokes shift (~1.5 - 1.7 eV) of the fluorescence are caused by a fast multi-step vibrational relaxation process of the excited molecule due to the collision with other gas phase molecules.^{35,36,41} These collisions induce the acetone molecule to relax within the excited electronic state to lower vibrational states and thus lead to the population of lower-energy S_1 states. The excited molecule can radiatively recombine from each of these energy levels to S_0 or relax further to lower-energy S_1 states after another collision (or cross to the triplet state) leading to an emission broadening and a shift towards lower energies. Comparative measurements in an acetone/ O_2/N_2 gas flow at room temperature also show the same broad blue emission at 420 nm as in the catalytic PL-tests at high temperatures (Figure S6).

In Figure 2b and d it was demonstrated that the acetone-related PL intensity and the acetone yield show a slightly different behavior at high temperatures (260 °C - 280 °C). The measured acetone yield starts to saturate above 250 °C, while in the PL investigations an intensity increase can be observed even at high temperatures. As a possible explanation of this discrepancy, one needs to consider that in the PL study reaction products are studied near the catalyst surface (as the

maximum pulse fluence is on the powder surface in the laser focus), whereas the acetone yield measurements have been performed at the reactor outlet. By examining the formation of acetone by PL spectroscopy directly at the surface after the catalytic process, a further conversion of acetone through oxidation can be avoided. This suggests that a possible cause of the drop in the acetone yield observed at temperatures close to 280 °C in Figure 2b is the further oxidation of acetone to H₂O and CO₂. However, it should be mentioned that the use of a reactor for the catalytic tests with a gas flow through the bed can lead to slight differences in the catalytic behavior compared to the reactor chamber for PL measurements with a gas flow over the bed.

The decisive prerequisite for the excitation of acetone and the observation of the blue acetone emission is the presence of *n* orbitals due to unbound electron pairs of the O-atom. Consequently, the observed emission at around 420 nm cannot occur if the molecule is still chemically bounded to the catalyst's surface. Therefore, we present the following model for the occurrence of the blue acetone emission during 2-propanol oxidation over Co₃O₄ (Scheme 1).



Scheme 1. Model describing the absorption and emission process of acetone molecules via the $n \leftrightarrow \pi^*$ transition of the carbonyl group in the 2-propanol oxidation over Co_3O_4 nanowires.

Various reaction schemes have been proposed in literature describing the underlying mechanism of 2-propanol oxidation and acetone formation over a metal (oxide) surface.⁴²⁻⁴⁴ For Co_3O_4 systems, the 2-propanol conversion is mostly explained by a dehydroxylation process with deprotonation of the alcohol group by a surface oxygen species, whereby an OH group is formed, while the remaining alkoxide is adsorbed on an active surface site.²⁷⁻²⁹ The active surface sites of Co_3O_4 to which 2-propoxide can bind are formed by Co^{3+} metal cations or Co^{3+} ensembles, respectively.^{28,29} The subsequent loss of another proton (H^+) and the desorption from the surface finally leads to the acetone formation. Only after the acetone split-off from the catalyst surface and the formation of a carbonyl group with unbound n orbitals, it is possible to optically excite the acetone molecule at 270 nm and detect the blue emission at ~ 420 nm. After desorption, the excited acetone molecule can be in the gas phase near the catalyst surface or physisorbed on the catalyst surface without a chemical bond.

Under working conditions, a catalysts surface including its adsorbates is subject to permanent changes, which has an impact on the catalytic reaction and activity. To determine the influence of TPO on the catalyst surface, Co_3O_4 nanowires are examined during the subsequent cooling process after a catalytic test has been carried out. For this purpose, the catalyst is heated up to 280 °C in a 2-propanol/ O_2/N_2 gas flow. This temperature is maintained for 1 hour and afterward the catalyst is cooled down to 50 °C (Figure 3). The examination using *in situ* PL measurements is again accompanied by catalytic measurements via gas chromatography under comparable conditions (see Supporting Information).

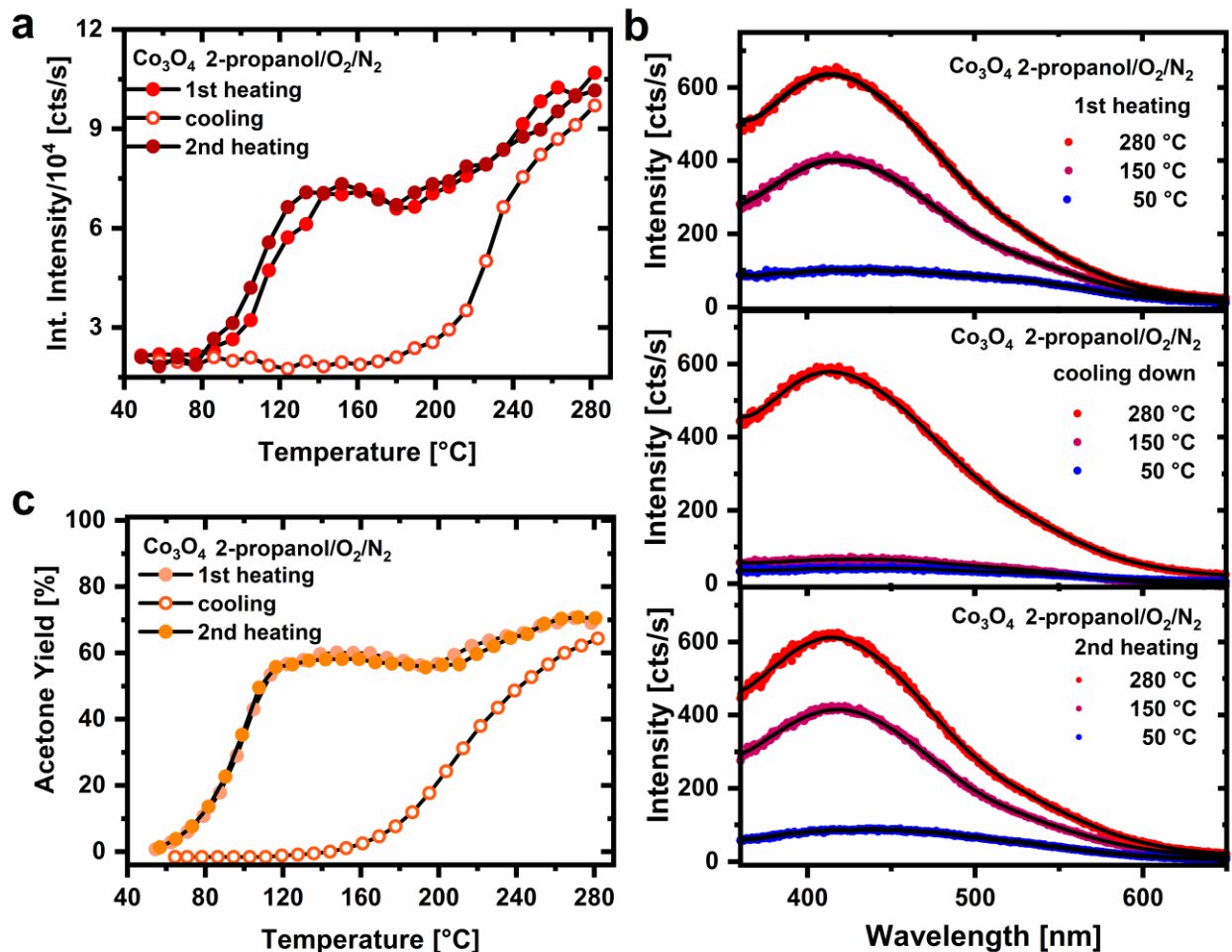


Figure 3. (a) and (b) cyclic PL study (1st heating, cooling down and 2nd heating) of the PL emission behavior of Co_3O_4 nanowires under UV excitation ($\lambda_{\text{exc}} = 270 \text{ nm}$, $\rho = 8.6 \mu\text{J}/\text{cm}^2$) and a constant 2-propanol/ O_2/N_2 gas flow. The temperature course of the integrated intensity (a) and the associated PL spectra (b) are shown. (c) Cyclic study of the 2-propanol oxidation over Co_3O_4 nanowires: Temperature-dependent yields of acetone under a constant 2-propanol/ O_2/N_2 gas flow. Before the 2nd heating process of the PL and acetone yield investigation, a TPO step is carried out.

During the first heating process, the formation of an intermediate maximum around 150 $^\circ\text{C}$ and a subsequent increase up to a temperature of 280 $^\circ\text{C}$ is demonstrated again for the PL intensity. However, during the subsequent cooling process the PL intensity drops steeply, and an

intermediate maximum is no longer detected. In fact, nearly no emission signal is observable anymore at 150 °C. An analogous temperature-dependent course is obtained during cooling when the acetone yield in the gas flow is determined, with complete deactivation of the catalyst below 150 °C (Figure 3c). The cause of the catalyst deactivation and the decrease in acetone formation is assumed to be the presence of adsorbates such as highly stable and strongly bound acetate or carbonaceous species on the Co₃O₄ surface.^{27–29} This leads to a decrease in free active surface sites at the catalyst surface. As a result, the formation of acetone decreases and thereby also the intensity of the blue emission.

To confirm this hypothesis, a second TPO is carried out to remove disturbing adsorbates and reoxidize the surface. The Co₃O₄ catalyst is therefore annealed under oxidative conditions up to a temperature of 280 °C after the cooling step. As a result, the same blue PL signal with a maximum at ~420 nm is detected again in the second heating step and the initial course of the PL intensity with an intermediate maximum around 150 °C is restored (Figure 3a and b). This can be confirmed by catalytic tests via gas chromatography showing the original temperature profile after performing a TPO step as well (Figure 3c). Thus, the surface of the Co₃O₄ nanowires catalyst can be successfully freed from adsorbates by performing an additional TPO step, thereby reactivating the catalyst.

In summary, we developed an *in situ* photoluminescence method to study the thermo-catalytic conversion of 2-propanol to acetone over mesostructured Co₃O₄ nanowires. A pretreatment of the catalyst with temperature programmed oxidation enables the catalytic reaction. By choosing a discrete excitation with a frequency-tripled Ti:sapphire laser ($\lambda_{\text{exc}} = 270 \text{ nm}$), acetone molecules

are selectively excited separately without interference by adsorbates or intermediate products. It is shown that the blue emission of acetone at ~ 420 nm can be used to monitor the temperature-dependent conversion of 2-propanol to acetone with an intermediate maximum at 150 °C and a further increase up to 280 °C. The steep drop in the PL intensity during the subsequent cooling process is explained by the catalyst deactivation due to disturbing byproducts such as acetate or carbonaceous species blocking active surface sites. A model is suggested describing the emission process of acetone during 2-propanol oxidation. The occurrence of the blue emission is assigned to the $\pi^* \rightarrow n$ transition of the carbonyl O-atom under the participation of unbound electrons. To the best of our knowledge, this is the first investigation of a thermo-catalytic process using *in situ* PL spectroscopy. With this new method, dynamic processes can be examined in real time and in direct proximity to the surface of heterogeneous catalyst systems. Due to the use of distinct excitation wavelengths, reaction products can be selectively excited and detected with high sensitivity.

ASSOCIATED CONTENT

Supporting Information

Experimental Methods, sample characterization of Co_3O_4 nanowires by XRD, TEM, nitrogen physisorption and Raman measurements, influence of TPO on Co_3O_4 surface coverage with OH/water (examined with PL spectroscopy and gas chromatography), Co_3O_4 emission behavior under oxidative conditions (with/without 2-propanol), optical absorption of acetone and 2-propanol as liquid and Co_3O_4 emission in acetone enriched O_2/N_2 gas flow.

AUTHOR INFORMATION

Corresponding Author

*E-mail: gerd.bacher@uni-due.de

Notes

The authors declare no competing financial interests.

ACKNOWLEDGMENT

This work was funded by the Deutsche Forschungsgemeinschaft (DFG, German Research Foundation) – Project number 388390466-TRR 247 within the collaborative research center/transregio 247 “Heterogeneous Oxidation Catalysis in the Liquid Phase” (projects A1, B3 and C1)) and Carbon2Chem project funded by the Bundesministerium für Bildung und Forschung (BMBF) of the German government. HT thanks Max Planck Society for the basic funding.

REFERENCES

- (1) Feng, K.; Wang, Y.; Guo, M.; Zhang, J.; Li, Z.; Deng, T.; Zhang, Z.; Yan, B. In-situ/operando techniques to identify active sites for thermochemical conversion of CO₂ over heterogeneous catalysts. *J. Energy Chem.* **2021**, *62*, 153–171.
- (2) Schlögl, R. Heterogeneous catalysis. *Angew. Chem. Int. Ed.* **2015**, *54*, 3465–3520.
- (3) Somorjai, G. A. Active Sites in Heterogeneous Catalysis. *Adv. Catal.* **1977**, *26*, 1–68.
- (4) Dou, J.; Sun, Z.; Opalade, A. A.; Wang, N.; Fu, W.; Tao, F. F. Operando chemistry of catalyst surfaces during catalysis. *Chem. Soc. Rev.* **2017**, *46*, 2001–2027.
- (5) Wang, Y.-H.; Zheng, S.; Yang, W.-M.; Zhou, R.-Y.; He, Q.-F.; Radjenovic, P.; Dong, J.-C.; Li, S.; Zheng, J.; Yang, Z.-L.; Attard, G.; Pan, F.; Tian, Z.-Q.; Li, J.-F. In situ Raman spectroscopy reveals the structure and dissociation of interfacial water. *Nature* **2021**, *600*, 81–85.
- (6) Haw J. F. *In-situ spectroscopy in heterogeneous catalysis*; Wiley-VCH: Weinheim, 2002.
- (7) Hunger, M.; Weitkamp, J. In situ IR, NMR, EPR, and UV/Vis Spectroscopy: Tools for New Insight into the Mechanisms of Heterogeneous Catalysis. *Angew. Chem. Int. Ed.* **2001**, *40*, 2954–2971.
- (8) Chakrabarti, A.; Ford, M. E.; Gregory, D.; Hu, R.; Keturakis, C. J.; Lwin, S.; Tang, Y.; Yang, Z.; Zhu, M.; Bañares, M. A.; Wachs, I. E. A decade+ of operando spectroscopy studies. *Catal. Today* **2017**, *283*, 27–53.
- (9) Hess, C. New advances in using Raman spectroscopy for the characterization of catalysts and catalytic reactions. *Chem. Soc. Rev.* **2021**, *50*, 3519–3564.
- (10) Lamberti, C.; Zecchina, A.; Groppo, E.; Bordiga, S. Probing the surfaces of heterogeneous catalysts by in situ IR spectroscopy. *Chem. Soc. Rev.* **2010**, *39*, 4951–5001.
- (11) Wachs, I. E. In situ Raman spectroscopy studies of catalysts. *Top. Catal.* **1999**, *8*, 57–63.
- (12) Wachs, I. E.; Roberts, C. A. Monitoring surface metal oxide catalytic active sites with Raman spectroscopy. *Chem. Soc. Rev.* **2010**, *39*, 5002–5017.
- (13) Burcham, L. J.; Deo, G.; Gao, X.; Wachs, I. E. In situ IR, Raman, and UV-Vis DRS spectroscopy of supported vanadium oxide catalysts during methanol oxidation. *Top. Catal.* **2000**, *11*, 85–100.
- (14) Hallac, B.; Brown, J.; Stavitski, E.; Harrison, R.; Argyle, M. In Situ UV-Visible Assessment of Iron-Based High-Temperature Water-Gas Shift Catalysts Promoted with Lanthana: An Extent of Reduction Study. *Catalysts* **2018**, *8*, 63.

- (15) Nijhuis, T. A.; Tinnemans, S. J.; Visser, T.; Weckhuysen, B. M. Operando spectroscopic investigation of supported metal oxide catalysts by combined time-resolved UV-VIS/Raman/on-line mass spectrometry. *Phys. Chem. Chem. Phys.* **2003**, *5*, 4361–4365.
- (16) Rodriguez, J. A.; Hanson, J. C.; Stacchiola, D.; Senanayake, S. D. In situ/operando studies for the production of hydrogen through the water-gas shift on metal oxide catalysts. *Phys. Chem. Chem. Phys.* **2013**, *15*, 12004–12025.
- (17) Zaera, F. In-situ and operando spectroscopies for the characterization of catalysts and of mechanisms of catalytic reactions. *J. Catal.* **2021**, *404*, 900–910.
- (18) Anpo, M.; Matsuoka, M.; Hano, K.; Mishima, H., Ono, T., Yamashita, H. Photocatalytic Decomposition of N₂O on Cu⁺/Y-Zeolite Catalysts prepared by Ion-Exchange. *Korean J. Chem. Eng.* **1997**, *14*, 498–501.
- (19) Anpo, M.; Matsuoka, M.; Yamashita, H.; Ju, W.-S.; Park, S.; Shul, Y. Photocatalytic Decomposition of NO on Transition Metal Ion-exchanged Zeolite Catalysts. *J. Ind. Eng. Chem.* **2000**, *6*, 133–143.
- (20) Röhr, J. A.; Sá, J.; Konezny, S. J. The role of adsorbates in the green emission and conductivity of zinc oxide. *Commun. Chem.* **2019**, *2*, 52.
- (21) van Dijken, A.; Meulenkamp, E. A.; Vanmaekelbergh, D.; Meijerink, A. The Kinetics of the Radiative and Nonradiative Processes in Nanocrystalline ZnO Particles upon Photoexcitation. *J. Phys. Chem. B* **2000**, *104*, 1715–1723.
- (22) Kortewille, B.; Pflingsten, O.; Bacher, G.; Strunk, J. Supported Vanadium Oxide as a Photocatalyst in the Liquid Phase: Dissolution Studies and Selective Laser Excitation. *ChemPhotoChem* **2021**, DOI: 10.1002/cptc.202100120.
- (23) Garcia, H.; Nieto, J. M. L.; Palomares, E.; Solsona, B. Photoluminescence of supported vanadia catalysts: linear correlation between the vanadyl emission wavelength and the isoelectric point of the oxide support. *Catal. Letters* **2000**, *69*, 217–221.
- (24) Klein, J.; Kampermann, L.; Saddeler, S.; Korte, J.; Kowollik, O.; Smola, T.; Schulz, S.; Bacher, G. Atmosphere-sensitive photoluminescence of Co_xFe_{3-x}O₄ metal oxide nanoparticles. *RSC Adv.* **2021**, *11*, 33905–33915.
- (25) Anpo, M.; Costentin, G.; Giamello, E.; Lauron-Pernot, H., Sojka, Z. Characterisation and reactivity of oxygen species at the surface of metal oxides. *J. Catal.* **2021**, *393*, 259–280.
- (26) Lozano, A.; Yip, B.; Hanson, R. K. Acetone: a tracer for concentration measurements in gaseous flows by planar laser-induced fluorescence. *Exp. Fluids* **1992**, *13*, 369–376.

- (27) Anke, S.; Bendt, G.; Sinev, I.; Hajiyani, H.; Antoni, H.; Zegkinoglou, I.; Jeon, H.; Pentcheva, R.; Roldan Cuenya, B.; Schulz, S.; Muhler, M. Selective 2-Propanol Oxidation over Unsupported Co_3O_4 Spinel Nanoparticles: Mechanistic Insights into Aerobic Oxidation of Alcohols. *ACS Catal.* **2019**, *9*, 5974–5985.
- (28) Anke, S.; Falk, T.; Bendt, G.; Sinev, I.; Hävecker, M.; Antoni, H.; Zegkinoglou, I.; Jeon, H.; Knop-Gericke, A.; Schlögl, R.; Roldan Cuenya, B.; Schulz, S.; Muhler, M. On the reversible deactivation of cobalt ferrite spinel nanoparticles applied in selective 2-propanol oxidation. *J. Catal.* **2020**, *382*, 57–68.
- (29) Falk, T.; Budiyanto, E.; Dreyer, M.; Pflieger, C.; Waffel, D.; Büker, J.; Weidenthaler, C.; Ortega, K. F.; Behrens, M.; Tüysüz, H.; Muhler, M.; Peng, B. Identification of Active Sites in the Catalytic Oxidation of 2-Propanol over $\text{Co}_{1+x}\text{Fe}_{2-x}\text{O}_4$ Spinel Oxides at Solid/Liquid and Solid/Gas Interfaces. *ChemCatChem* **2021**, *13*, 2942–2951.
- (30) Budiyanto, E.; Yu, M.; Chen, M.; DeBeer, S.; Rüdiger, O.; Tüysüz, H. Tailoring Morphology and Electronic Structure of Cobalt Iron Oxide Nanowires for Electrochemical Oxygen Evolution Reaction. *ACS Appl. Energy Mater.* **2020**, *3*, 8583–8594.
- (31) Deng, X.; Chen, K.; Tüysüz, H. Protocol for the Nanocasting Method: Preparation of Ordered Mesoporous Metal Oxides. *Chem. Mater.* **2017**, *29*, 40–52.
- (32) Stoyanovskii, V. O.; Snytnikov, V. N. Laser-induced luminescence associated with surface hydroxide groups in Al_2O_3 . *Kinet. Catal.* **2009**, *50*, 450–455.
- (33) Kampermann, L.; Klein, J.; Korte, J.; Kowollik, O.; Pflingsten, O.; Smola, T.; Saddeler, S.; Piotrowiak, T. H.; Salamon, S.; Landers, J.; Wende, H.; Ludwig, A.; Schulz, S.; Bacher, G. Link between Structural and Optical Properties of $\text{Co}_x\text{Fe}_{3-x}\text{O}_4$ Nanoparticles and Thin Films with Different Co/Fe Ratios. *J. Phys. Chem. C* **2021**, *125*, 14356–14365.
- (34) Lukashuk, L.; Yigit, N.; Rameshan, R.; Kolar, E.; Teschner, D.; Hävecker, M.; Knop-Gericke, A.; Schlögl, R.; Föttinger, K.; Rupprechter, G. Operando Insights into CO Oxidation on Cobalt Oxide Catalysts by NAP-XPS, FTIR, and XRD. *ACS Catal.* **2018**, *8*, 8630–8641.
- (35) Schulz, C.; Sick, V. Tracer-LIF diagnostics: quantitative measurement of fuel concentration, temperature and fuel/air ratio in practical combustion systems. *Prog. Energy Combust. Sci.* **2005**, *31*, 75–121.
- (36) Thurber, M. C.; Grisch, F.; Kirby, B. J.; Votsmeier, M.; Hanson, R. K. Measurements and modeling of acetone laser-induced fluorescence with implications for temperature-imaging diagnostics. *Appl. Opt.* **1998**, *37*, 4963–4978.
- (37) Hansen, D. A.; Lee, E. K. C. Radiative and nonradiative transitions in the first excited singlet state of symmetrical methyl-substituted acetones. *J. Chem. Phys.* **1975**, *62*, 183–189.

- (38) Pischel, U.; Nau, W. M. Switch-over in photochemical reaction mechanism from hydrogen abstraction to exciplex-induced quenching: interaction of triplet-excited versus singlet-excited acetone versus cumyloxyl radicals with amines. *J. Am. Chem. Soc.* **2001**, *123*, 9727–9737.
- (39) Grossmann, F.; Monkhuose, P. B.; Ridder, M.; Sick, V.; Wolfrum, J. Temperature and pressure dependences of the laser-induced fluorescence of gas-phase acetone and 3-pentanone. *Appl. Phys. B: Lasers and Optics* **1996**, *62*, 249–253.
- (40) Lind, S.; Trost, J.; Zigan, L.; Leipertz, A.; Will, S. Application of the tracer combination TEA/acetone for multi-parameter laser-induced fluorescence measurements in IC engines with exhaust gas recirculation. *Proc. Combust. Inst* **2015**, *35*, 3783–3791.
- (41) Thurber, M. C.; Hanson, R. K. Pressure and composition dependences of acetone laser-induced fluorescence with excitation at 248, 266, and 308 nm. *Appl. Phys. B: Lasers and Optics* **1999**, *69*, 229–240.
- (42) Foo, G. S.; Polo-Garzon, F.; Fung, V.; Jiang, D.; Overbury, S. H.; Wu, Z. Acid–Base Reactivity of Perovskite Catalysts Probed via Conversion of 2-Propanol over Titanates and Zirconates. *ACS Catal.* **2017**, *7*, 4423–4434.
- (43) Akiba, E.; Soma, M.; Onishi, T.; Tamaru, K. The Mechanism of the Decomposition Reaction of 2-propanol on ZnO. *Z. Phys. Chem.* **1980**, *119*, 103–110.
- (44) Gong, J.; Flaherty, D. W.; Yan, T.; Mullins, C. B. Selective oxidation of propanol on Au(111): mechanistic insights into aerobic oxidation of alcohols. *ChemPhysChem* **2008**, *9*, 2461–2466.